J Bioenerg Biomembr (2007) 39:99–107
DOI 10.1007/s10863-006-9066-6

ORIGINAL PAPER

Chemical modification of mono-cysteine mutants allows a more global look at conformations of the ε subunit of the ATP synthase from *Escherichia coli*

Sangeeta Ganti · Steven B. Vik

Received: 28 September 2006 / Accepted: 31 October 2006 / Published online: 23 February 2007

Abstract The ε subunit of the ATP synthase from *E. coli* undergoes conformational changes while rotating through 360° during catalysis. The conformation of ε was probed in the membrane-bound ATP synthase by reaction of mono-cysteine mutants with 3-N-maleimidyl-propionyl biocytin (MPB) under resting conditions, during ATP hydrolysis, and after inhibition by ADP-AlF_3. The relative extents of labeling were quantified after electrophoresis and blotting of the partially purified ε subunit. Residues from the N-terminal β-sandwich domain showed a position-specific pattern of labeling, consistent with prior structural studies. Some residues near the ε-γ interface showed changes up to two-fold if labeling occurred during ATP hydrolysis or after inhibition by ADP-AlF_3. In contrast, residues found in the C-terminal α-helices were all labeled to a moderate or high level with a pattern that was consistent with a partially opened helical hairpin. The results indicate that the two C-terminal α-helices do not adopt a fixed conformation under resting conditions, but rather exhibit intrinsic flexibility.

Keywords ATP synthase · ε subunit · Conformational change · Cysteine · Mutagenesis · Chemical modification · 3-N-maleimidyl-propionyl biocytin (MPB)

Abbreviations FRET: Fluorescence resonance energy transfer · LDAO: Lauryl dimethyl amine oxide · MPB: 3-*N*-maleimidyl-propionyl biocytin · TFPAM-3: (*N*-(4-azido-2,3,5,6-tetrafluorobenzyl)-3-maleimido-propionamide)

S. Ganti · S.B. Vik (✉)
Department of Biological Sciences, Southern Methodist University, Dallas, TX 75275-0376, USA
e-mail: svik@smu.edu

Introduction

The ATP synthase is a membrane-bound, multi-subunit, rotary motor for the synthesis of ATP. It is typically found in the membranes of mitochondria, chloroplasts and bacteria (For recent reviews see (Capaldi and Aggeler, 2002; Ackerman and Tzagoloff, 2005; Dimroth et al., 2006). The enzyme from *E. coli* is somewhat simpler than those from mitochondria, but it preserves the essential features. Three subunits make up the rotor: γ, ε and the oligomeric ring of *c* subunits. The five types of stator subunits include 3 copies of α and β, which together form the three catalytic and three non-catalytic nucleotide binding sites. These subunits are connected to the membrane via δ, *b* and *a* subunits, which form the so-called peripheral stalk. The single *a* subunit makes an interface with the rotary *c* subunits, and these subunits work together to translocate protons. The role of the γ subunit is to communicate the effects of rotation to the catalytic sites, so that the conformations of all three sites change in sequence to accommodate substrate binding, phosphorylation and product release. This is described by the "binding change" mechanism (Boyer, 1993).

The *E. coli* F_1F_o ATP synthase catalyzes both ATP driven proton translocation and proton-gradient-driven ATP synthesis. The role of the ε subunit is unclear, but it has long been known that it inhibits ATP hydrolysis in both F_1 and F_1F_o enzymes (Smith and Sternweiss, 1977; Kato-Yamada et al., 1999; Peskova and Nakamoto, 2000; Feniouk et al. 2006). Evidence has been presented that the ε subunit from the thermophilic bacterium *Bacillus PS3* binds ATP directly (Kato-Yamada and Yoshida, 2003; Iizuka et al., 2006). ε is also known to rotate through 360° during ATP hydrolysis (Bulygin et al., 1998; Kato-Yamada et al., 1998). The structure of the isolated ε subunit has been analyzed by both X-ray crystallography (Uhlin et al., 1997) and NMR

(Wilkens et al., 1995; Wilkens and Capaldi, 1998), with both methods revealing a nearly identical two-domain structure. An alternative conformation was revealed (Rodgers and Wilce, 2000) when ε was co-crystallized with the globular domain of the γ subunit, called γ'. A similar conformation was found for ε in a low-resolution structure of the *E. coli* F_1 ATPase (Hausrath et al., 2001). A variety of studies employing proteolysis (Mendel-Hartvig and Capaldi, 1991a,b), antibody binding (Johnson and McCarty, 2002), cross-linking (Aggeler et al., 1992, 1995; Suzuki et al., 2003), and FRET (Iino et al., 2005) have shown ε to exist in different conformations, generally described as compact and extended conformations. In the compact conformation, the two α-helices of the C-terminal domain are folded together in a helical hairpin and are close to the *N*-terminal β-sandwich domain. This is the conformation seen in the isolated ε subunit, and also that of the mitochondrial homolog as found in the F_1 ATPase (Gibbons et al., 2000). In the extended conformation, the hairpin comes undone and the two C-terminal α-helices are extended, nearly end to end. The details of this conformation are unclear, since it has only been seen in a crystal form with a truncated γ subunit. Furthermore, there may be several different extended conformations with the C-terminus of ε docked at different sites in the intact enzyme.

This study was undertaken to see if one of the previously identified conformations of ε could be confirmed in the intact, membrane-bound ATP synthase. To probe the conformation of ε throughout its polypeptide chain, over twenty mono-cysteine mutants were constructed, and reacted with the thiol reagent MPB. The pattern of labeling was not entirely in agreement with the conformation of either the isolated ε subunit or with that of the γ'-ε co-crystal, but was consistent with intrinsic flexibility of at least one of the C-terminal α-helices.

Materials and methods

Materials

Restriction endonucleases were obtained from New England Biolabs, (Beverly, MA). Synthetic oligonucleotides were obtained from Operon Technologies, (Huntsville, AL). DNA sequencing was done by Lone Star Labs, (Houston, TX). MPB was obtained from Molecular Probes-Invitrogen (Eugene, OR). Reagents for electrophoresis, immunoblotting and isoelectric focusing were obtained from Bio-Rad (Hercules, CA). Anti-ε monoclonal antibodies were a generous gift from Dr. Roderick Capaldi, University of Oregon.

Plasmids, mutagenesis, growth and expression

Plasmids pXH302S (Xiong and Vik, 1995a,b), pSA302S and pSG302S were used for construction of mutants. Plasmid pSA302S was constructed from pXH302S by digesting with *Nco* I and *AsiS* I, and ligating the large fragment to an 87 base pair fragment of synthetic DNA. This introduced four new unique restrictions sites in the gene for ε: *Blp* I, *Xho* I, *Acc* I and *Eag* I for constructing mutations in residues 95–116. Plasmid pSG302S was constructed from pSA302S by inserting a 49 base pair fragment of synthetic DNA at the *AsiS* I site. This regenerated the 3′ end of the gene, introduced unique *Mlu* I and *Nsi* I restriction sites, and by the use of degenerate nucleotides, allowed the construction of both a wild type coding sequence, and one with an extra cysteine at position 138. This construct was used for mutations at residues 120–138. Amino acid substitutions were introduced using cassette mutagenesis (Vik et al., 1988; Xiong and Vik, 1995a,b). For expression, XH1 (*uncC*, *bglR*, *thi-1*, *rel-1*, *Hfr Po1*) was used as the background strain (Xiong and Vik, 1995a,b). It produced no subunit ε due to a deletion of 273 bp from –2 to 271 in the *uncC* gene, and was complemented by plasmids containing a wild type *uncC* gene.

Preparation, labeling, and stripping of membrane vesicles

Membrane vesicles were prepared as described previously (Long et al., 2002), and resuspended in 10 ml of 200 mM Tris-HCl pH 8.0 for labeling experiments. To prepare stripped membrane vesicles (loss of F_1), the membrane vesicles were resuspended in low ionic strength buffer, 1 mM Tris-HCl, pH 8.0, 0.5 mM EDTA, 10% glycerol (v/v) and 2.5 mM β-mercaptoethanol, followed by centrifugation at 200,000 $\times$ *g* for 1 h at 4°C. Rates of ATP hydrolysis were measured by a coupled-enzyme assay, as described previously (Xiong and Vik, 1995a,b). For labeling experiments, membrane vesicles were incubated in 200 mM Tris-HCl (pH 8.0) with 120 μM MPB at room temperature for 20 min. Longer incubations under these conditions did not result in a greater extent of labeling. The reaction was stopped by addition of β-mercaptoethanol to a final concentration of 20 mM. The sample was centrifuged for 1 hr at 200,000 $\times$ *g* and the pellet obtained was suspended in stripping buffer and centrifuged again. For inhibition by ADP-AlF3, the procedure of Braig et al was followed (Braig et al., 2000). All mutants were inhibited at least 90% in ATP hydrolysis by this treatment. For labeling in the presence of ATP, the membrane vesicles were resuspended in 200 mM Tris-HCl (pH 8.0), with 3 mM ATP and 1 mM $MgSO_4$. To this suspension, MPB was added and incubated as described above.

Analysis

ε subunit was purified by isoelectric focusing electrophoresis using a Bio-Rad MiniRotofor® cell, essentially as described earlier (Xiong and Vik, 1995a,b). Fractions were analyzed

on two 4–15% polyacrylamide gradient gels followed by transfer to polyvinyledine difluoride membranes. One blot was developed using an alkaline phosphatase-avidin conjugate for detection of MPB labeling, while the second was probed using anti-ε monoclonal antibody, as described previously (Zhang and Vik, 2003). This antibody appeared to bind strongly to all of the mutants reported here. The intensity of the bands for each mutant were quantified using the software Image J (freely available at http://rsb.info.nih.gov/ij). These values were divided by the quantity of labeling found in an immunoblot from the same amount of material. These scaled values were then compared to the corresponding values of mutants 28, 55 or 120 that appeared on the same blot. Two to five determinations were used to calculate an average and standard deviation for each mutant. The highest labeling mutant, H58C, was set at a value of 100. Accessible surface areas of the individual residues of ε were calculated using the Analytic Surface Calculation Package (Eisenhaber and Argos, 1993) through the IMP Bioinformatics Group server (http://mendel.imp.ac.at/mendeljsp/studies/asc.jsp).

Results

Twenty-three mono-cysteine mutations were constructed in the ε subunit of the ATP synthase using several different plasmids, and are listed in Table 1. Mutant 138C has a cysteine added to the C-terminus of the normal protein. Each plasmid was then used to transform the ε-deletion strain XH1. All of the resulting strains could grow on succinate minimal medium, indicating a functional ATP synthase. The sites chosen for mutation were surface residues of the N-terminal β-sandwich domain, or were residues throughout the C-terminal α-helical domain. The locations of the mutated residues are shown in Fig. 1. The face of the isolated ε as shown in panel B is expected to be largely shielded by the γ subunit, on the basis of the crystal structure of the mitochondrial F_1 (Gibbons et al., 2000). The face shown in panel C is expected to be more accessible.

To investigate the surface accessibility of each of the cysteine mutations, membrane vesicles were prepared from cultures of each mutant. Samples were reacted with 120 μM MPB for 20 min at room temperature. The membranes were stripped of F_1 by a low ionic strength wash, and the ε subunit was partially purified by subjecting the supernatant fraction to preparative isoelectric focusing. Equal volumes of fractions containing the ε subunit were loaded onto two polyacrylamide gels. One gel was used to detect the amount of chemical labeling, and the other was used to quantify the amount of ε subunit by immunoblotting. Representative experiments are shown in Fig. 2, for V112C, Q116C, and E120C. Panel A shows the extent of labeling, while panel B is an immunoblot, indicating the amount of ε subunit. By loading multiple samples on a single gel, and using several mutants as internal standards, relative extents of labeling were obtained for all of the mutants, as shown in Fig. 3. The highest extent of labeling, that of residue H58C, was set to 100 units.

The labeling of residues in the *N*-terminal domain, 17–81, varies from about one unit to 100 units, and it correlates well with the location of the residues with respect to the γ subunit, as seen in the γ'-ε co-crystal. Residue 79 is buried at the γ-ε interface, and L79C shows essentially no labeling. Residues 55, 56 and 58 are both exposed and distant from γ, and these mutants had the highest levels of label. Residues 17, 26, 28 and 81 are all near the γ subunit, and the corresponding cysteine mutants show rather low labeling, 10–25% of the maximum. In contrast, all 15 cysteine mutants in the C-terminal domain were labeled to the extent of 30–90% of maximum, indicating that none of the residues are inaccessible to the reagent.

To test whether the cysteine mutations had generally perturbed the conformation of the ε subunit, the effects of lauryl dimethyl amine oxide (LDAO) on ATP hydrolysis were measured. Under the conditions used here for ATP hydrolysis, the presence of 2% LDAO will stimulate ATP hydrolysis rates by 2–3 fold (Xiong and Vik, 1995a,b; Xiong et al., 1998). This indicates the extent of inhibition by the ε subunit. ATP hydrolysis by the wild type membranes was stimulated 2.1-fold, and nineteen of the mutants were in the range of 1.3–3.5 fold stimulation. E120C was stimulated 3.8-fold, and Q127C was stimulated 5.4-fold. Therefore, only one of the mutants exhibited a significantly greater extent of inhibition by ε, which might be consistent with an altered conformation.

The experimentally determined levels of labeling were compared with the exposure of residues as seen in two crystal structures, by first calculating the surface accessible areas for the residues that were mutated to cysteine (Eisenhaber and Argos, 1993). These values were then normalized by dividing by the surface area of that amino acid as calculated in

Table 1 Location of cysteine substitutions in the ε subunit

Residue number[a]	Domain	Plasmid[b]
17, 26, 28, 55, 56, 58, 79, 81	N-terminal	pXH302S (Xiong and Vik, 1995a,b)
94, 95, 97, 101, 104,	C-terminal, helix 1	pSA302S (This paper)
109, 110, 111	C-terminal, turn	pSA302S (This paper)
112, 116, 120	C-terminal, helix 2	pSA302S (This paper)
127, 131, 138	C-terminal, helix 2	pSG302S (This paper)

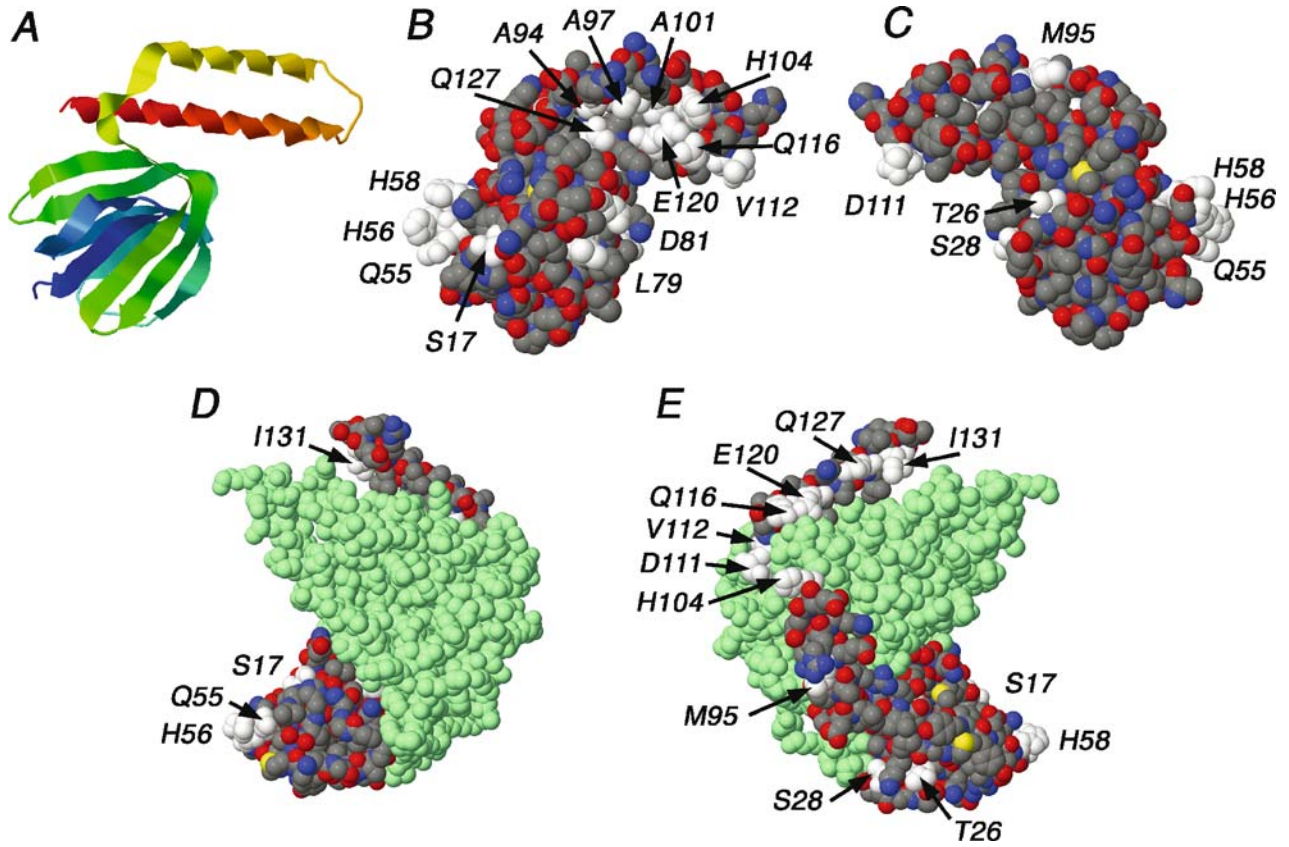

Fig. 1 (A) This is a ribbons-view of the isolated ε, showing the two domain structure: an N-terminal 10-stranded β-sandwich, and a C-terminal α-helical hairpin. (B) A spacefilling-view of ε in the same orientation as panel A. Mutated residues are colored white, while the rest of ε is in CPK colors: oxygen red, nitrogen blue, carbon gray, and sulfur yellow. In analogy with the mitochondrial enzyme, this face of ε is most likely to interact with the γ subunit. (C) This image is the same as in panel B after a rotation of 180 degrees about a vertical axis. (D) A spacefilling view of the γ'-ε complex. γ' is colored green and ε is colored as in panel B. The N-terminal domain of ε is in approximately the same orientation as in panel B. (E) This image is that of panel D after a rotation of 180 degrees about a vertical axis. Protein databank file 1aqt (Uhlin et al., 1997) was used in panels A–C, and 1fs0 (Rodgers and Wilce, 2000) was used in panels D and E. The Jmol application (freely available at http://www.jmol.org) was used to generate the images

a tripeptide (Chothia, 1976). The two crystal structures used were the isolated ε subunit, protein databank file 1aqt (Uhlin et al., 1997), and the γ'-ε hetero-dimer, protein databank file 1fs0 (Rodgers and Wilce, 2000). These calculated values, along with the normalized values from labeling shown in Fig. 3, are plotted in Fig. 4. Panel A shows the N-terminal mutants, and panel B shows the C-terminal mutants. Labeling by MPB is shown in the solid black bars, the surface accessibility of residues in the isolated ε subunit is shown in the white bars, and the surface accessibility of residues in the γ'-ε complex is shown in the shaded bars.

In the N-terminal region (Fig. 4A), there is a general correlation between labeling seen and the calculated surface accessibility in the γ'-ε complex, with the exception of residue 17. The extent of labeling of S17C is much less than would be predicted by the crystal structures. In the case of residues 79 and 81, both are highly exposed in the isolated ε structure, but are nearly buried in the γ'-ε complex, and the labeling matches that of the latter, suggesting that γ is shielding those residues from the MPB.

In the C-terminal region (Fig. 4B), the results are more complex. Residues 94, 97 and 117 are all alanine with little-to-no accessibility in both crystal forms, but the cysteine mutants can all be labeled to about 30–35%. In all of the other mutants, with the possible exception of H104C, the extent of labeling matches that of the crystal form with the greater accessibility. For example, V112C has high accessibility in the isolated ε, but not in the γ'-ε complex, and I131C has high accessibility in the γ'-ε complex, but not in the isolated ε. Both mutants show rather high labeling, with an extent of 55–60%.

A variety of earlier studies had indicated that the conformation of ε was sensitive to the presence of adenine nucleotides (Mendel-Hartvig and Capaldi, 1991a,b; Kato-Yamada et al., 2000). Therefore, the labeling of selected residues was carried out in the presence of Mg-ATP, and after inhibition by Mg-ADP-AlF_3. The first case represents the condition of ATP hydrolysis, and the second represents inhibition by a transition state analog. A summary of these results is presented in Fig. 5.

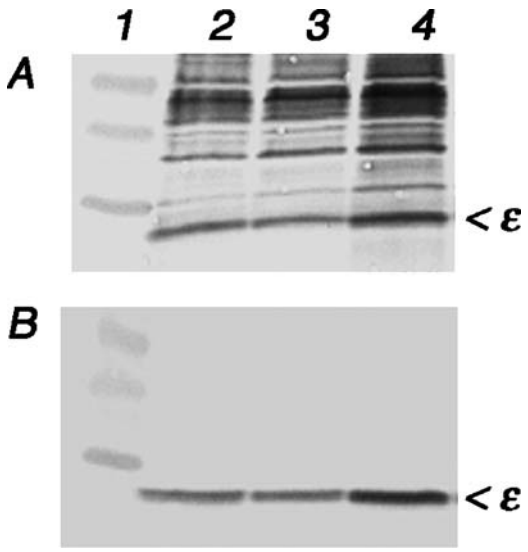

Fig. 2 A representative labeling experiment: MPB labeling of V112C, Q116C, and E120C. (A) MPB labeling: Lane 1, molecular weight standards 20, 29, and 37 kilodaltons. Lane 2, V112C. Lane 3, Q116C. Lane 4, E120C. (B) Immunoblots of the samlples in panel A: Lane 1, molecular weight standards 20, 29, and 37 kilodaltons. Lane 2, V112C. Lane 3, Q116C. Lane 4, E120C. Migration of the ε subunit is indicated at the right

The effect of labeling during ATP hydrolysis (Fig. 5A) is that the labeling of residue 17 increases by about 50%, and the labeling of residues 26 and 28 decreases up to two-fold. Other residues, including all those in the C-terminal region, are not affected. The effect of the ADP-AlF_3- inhibited state on labeling is shown in Fig. 5B. Under these conditions the labeling of S17C increased two-fold, while most of the other residues decreased slightly. The labeling of residues 26, 28, 111, and 131 decreased by about two-fold.

Discussion

No high resolution structure exists for the ε subunit from *E. coli* when it is found in an intact F_1 or F_1F_o ATP synthase complex. A crystal structure of the bovine mitochondrial F_1 shows the homologous subunit in a compact form (Gibbons et al., 2000), much as the isolated ε subunit from *E. coli* (Uhlin et al., 1997). However, mitochondria have an additional subunit in F_1 that interacts with the subunit that is homologous to ε, and so the situation is different. For example, studies of the rat liver enzyme (Pan et al., 1998) have shown that the homologous subunit is highly resistant to treatments of detergent and proteases. The goal of this work was to investigate the conformation of the subunit ε in a membrane-bound, functional enzyme. The conformation of ε was probed by testing the accessibility of more than twenty residues to chemical labeling. The labeling results in the resting enzyme were compared to the amino acid exposures calculated from both the crystal structures, isolated ε

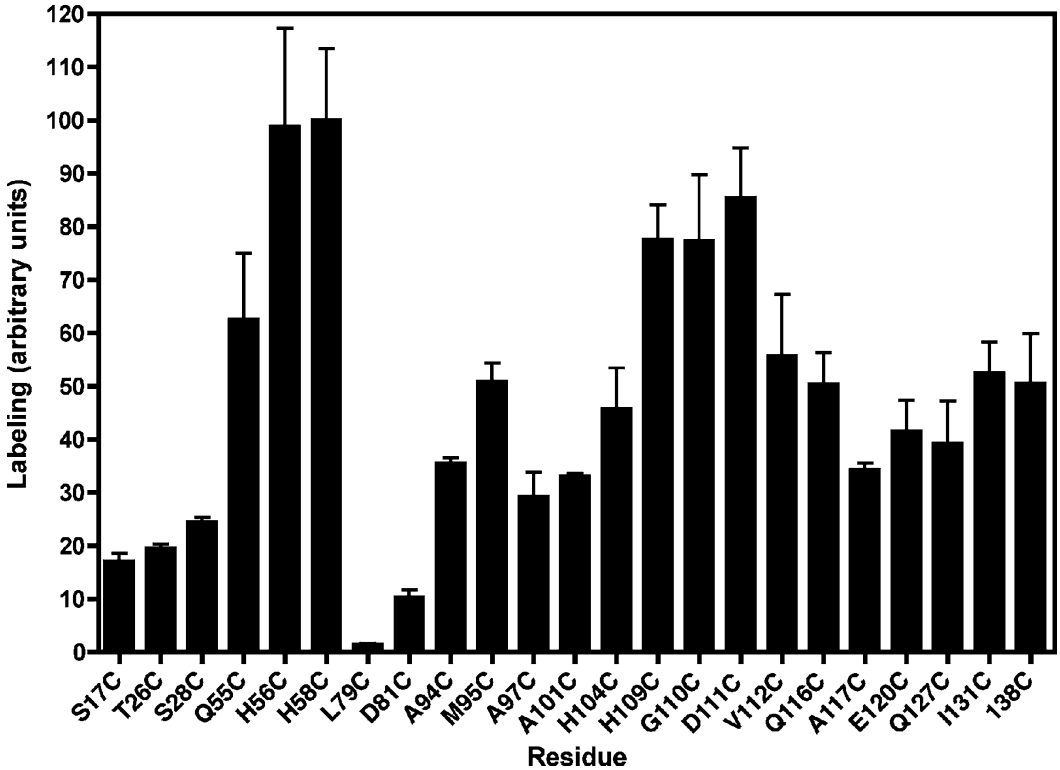

Fig. 3 Relative MPB labeling of twenty-three monocysteine mutants. The highest level of labeling, as described in the methods, that of H58C was set to 100 units. Each mutant was analyzed 2–5 times and the error bars represent the standard deviations of those measurements

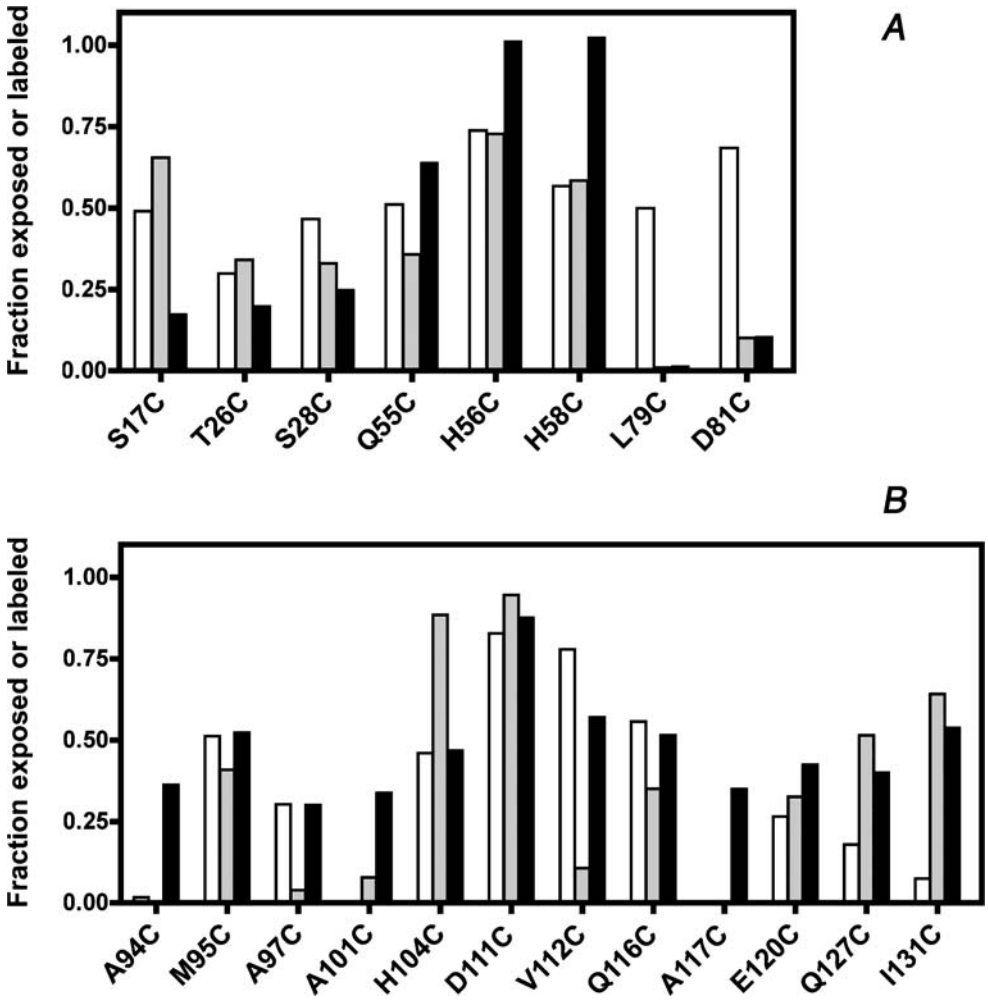

Fig. 4 Comparison of the MPB labeling with the surface accessibilities of the mutated residues as seen in two crystal structures. The *white bars* represent the fraction of residue that is exposed in the isolated ε structure (pdb 1aqt) (Uhlin et al., 1997). The shaded bars represent the fraction of each residue that is exposed in the γ'-ε structure (pdb 1fs0) (Rodgers and Wilce, 2000). The *black bars* represent the MPB labeling relative to that of the highest labeled residue 58. The data are taken from Fig. 3. (A) *N*-terminal residues 17–81. (B) C-terminal residues 95–131. Three residues are not included: 109 and 110, because they do not appear in the γ'-ε co-crystal structure, and 138, because it is an additional residue at the C-terminus and so it does not appear in either crystal form

and the γ'-ε co-crystal. The results were not consistent with either of the indicated conformations, but rather suggest an intrinsically flexible C-terminal domain.

Residues in the N-terminal domain of ε include S17, T26, S28, Q55, H56, H58, L79 and D81. The accessible surface area of residue S17 as calculated from the isolated ε structure is about 50%, and in the γ-ε structure is about 65%, but the extent of labeling is only about 15%. Since labeling is done in the intact enzyme, other subunits could contribute, directly or indirectly, to shielding residue 17. Furthermore, labeling increases both with addition of ATP and under conditions of ADP-AlF_3 inhibition, suggesting that conformational changes may have occurred at the γ-ε interface, leading to greater exposure of this residue. Previously, Capaldi and coworkers (Aggeler et al., 1992) had reported that S10C, which is adjacent to S17, cross-links to γ after reaction with the bi-functional cross-linker TFPAM-3. Furthermore, the yield of γ-ε cross-link increased 2-fold in the presence of ATP. These results support the view that residues in this region of ε are found at the γ-ε interface and that they undergo subtle changes in accessibility due to changes in nucleotide occupancy at catalytic sites.

Residues 26 and 28 have moderate accessibility (30–50%) in both crystal structures, γ'-ε and isolated ε. For both residues, the relative labeling was somewhat low (20–25%). Both residues showed decreased labeling in the presence of both ATP and ADP-AlF_3 as compared to the resting state. This region was proposed to be at the γ-ε-c interface (Rodgers and Wilce, 2000). Disulfide cross-linking experiments have reported that E31C and several other residues in this region could form disulfide cross-links to D42C of the c subunit (Zhang and Fillingame, 1995; Schulenberg et al.,

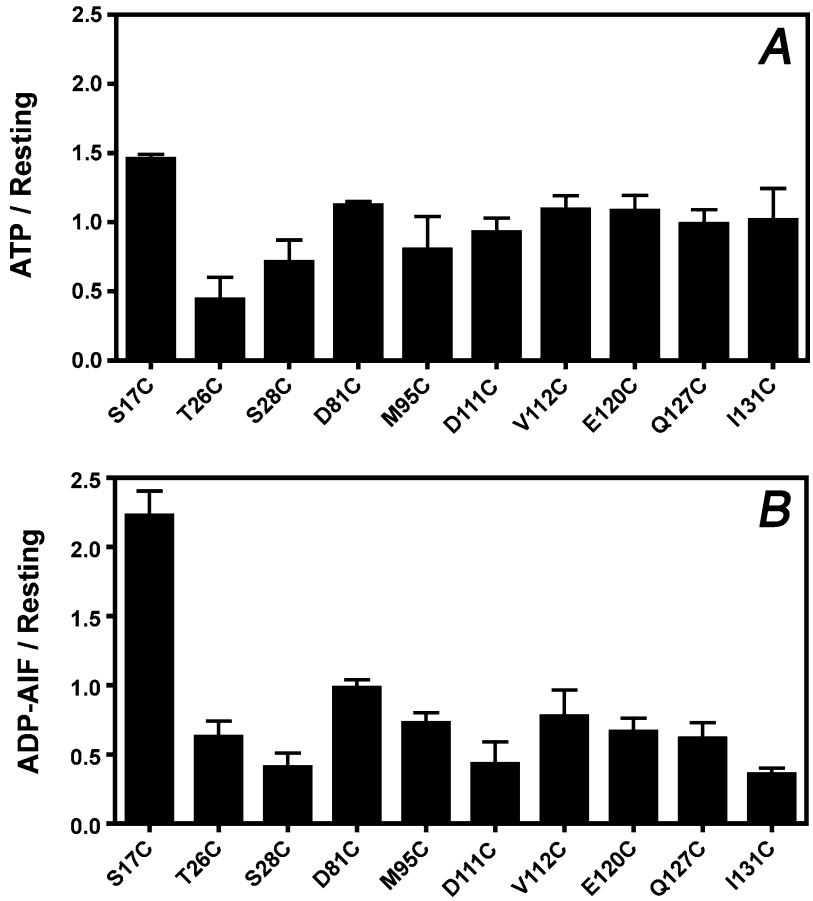

Fig. 5 Labeling of selected mutants in the presence of ATP, or after inhibition with ADP-AlF_3. (A) MPB labeling was carried out in the presence of 3 mM ATP, 1 mM $MgCl_2$. (B) MPB labeling was carried out after inhibition by ADP-AlF_3. Each mutant was analyzed 2–3 times, and the standard deviations are indicated by error bars

1999). The decreased labeling of 26 and 28 in the presence of nucleotides might be due to increased shielding by either γ or *c* subunits.

Residues 55, 56 and 58 of the *N*-terminal domain show maximal labeling and are not effected by nucleotide binding at the catalytic sites (data not shown). These residues show moderate to high accessible surface area in both crystal forms, and the high level of labeling indicates they are not shielded by any other subunit in the F_1F_o complex.

Residue 79 does not label above background levels. This pattern is consistent with the γ'-ε crystal structure, in which residue 79 is buried at the γ-ε interface. The lack of change in labeling during ATP hydrolysis or ADP-AlF_3 inhibition (data not shown) indicates that this is a part of a fixed interface. Labeling of 81 also matches its accessible surface area in the γ'-ε crystal structure. Residue 81 appears to be part of the hinge between the two domains, rather than at a fixed interface. The very low labeling suggests that this residue and by extension, the adjacent helix 1 (residues 90–106), are relatively immobile in the resting state.

With respect to the C-terminal domain of ε, the labeling patterns seen did not totally support either the compact conformation seen in the isolated ε, or the extended structure seen in the γ'-ε structure. In the compact conformation seen in the isolated ε, the second helix (112–135) shields the first helix (90–106). In particular, residues 94 and 101 are completely buried. Other residues, including 95, 97 and 104 are moderately exposed. As found in the γ'-ε crystal structure, in which the α-helices take up different positions relative to γ and to the *N*-terminal domain of ε, both 94 and 101 remain buried but have different positions. Residue 97 is also buried, residue 95 maintains the same accessibility and residue 104 is much more exposed. In contrast, the labeling pattern is similar for all five residues in the resting state. Therefore, the labeling pattern is not consistent with either of the two conformations shown in crystal structure, but would be consistent with an ε subunit in which helix 2 at the C-terminus is transiently moving away from its partner helix 1. In this group only residue 95 was tested extensively in the presence of nucleotides, and no significant differences were seen in the labeling.

The loop region between the two C-terminal α-helices, including residues 109–111, is highly exposed in the isolated ε subunit, and all three residues label well in the resting state of the F_1F_o enzyme. In the γ'-ε crystal structure, only

residue D111 of the loop is visible, and it has high accessibility. Labeling of residue D111 in the presence of ADP-AlF_3 was reduced by 50% relative to the resting state. This suggests that the restricted motion of the inhibited state might lower the accessibility of this residue. In previous studies, residue 108 has been cross-linked to both α and β subunits (Dallmann et al., 1992; Aggeler and Capaldi, 1996). It is possible that α or β subunits partially shield residue D111 in the ADP-AlF_3 bound state.

The residues of the second helix (112–135) and including the C-terminal 138, also labeled well in all cases, and the labeling pattern does not match the accessibility pattern of this helix in either crystal structure. In fact, the labeling pattern tends to match the exposure of the residues in their more accessible state. For example, V112 has low accessible surface area in the γ'-ε structure (11%) and high accessible surface area in the isolated ε structure (78%) and it labels well (66%). Likewise, I131 has high accessible surface area in the γ'-ε structure (70%) and low accessible surface area in the isolated ε structure (7%), but it also labels well (62%).

In the case of A117, it has less than 1% exposure in both crystal structures, but still labels at about 40% of maximum. In all, the labeling results of the second helix in the C-terminal domain of ε support the view that helix 2 of the coiled-coil comes apart transiently from helix 1. This would increase accessibility of most or all of the residues in these helices. None of the residues tested (112, 120, 127 and 131) had altered labeling in the presence of ATP, suggesting that they do not become more exposed during ATP hydrolysis. In the presence of the transition state analog ADP-AlF_3, I131 showed the greatest effect during labeling, about a 50% reduction. This might reflect increased shielding by the α or β subunits, or immobilization of helix 2.

Other studies have indicated the proximity of the C-terminus of ε to α and β subunits. A cross-link from 138C in ε to the β subunit was identified using the TFPAM-3 cross-linker (Tang and Capaldi, 1996). More recently Yoshida's group has shown in the thermophilic *Bacillus PS3* ATP synthase, that the C-terminus of ε forms a disulfide with the N-terminus of γ during ATP synthesis conditions (Suzuki et al., 2003). This latter position would be rather well-shielded from solution by the α and β subunits.

How do the labeling methods here compare to other approaches that have been used to probe conformational changes in ε? Chemical labeling requires a residue to be exposed to the reagent for a time sufficient for that chemical reaction to occur. In cross-linking, two residues must be in close proximity for a sufficient time, but do not probe conformational changes more generally. It may also be difficult to distinguish between residues that are in a fixed proximity, and those which occasionally are in close proximity during the period of the experiment. On the other hand, evidence of cross-linked products does not preclude additional conformational states. FRET measurements can be complementary to cross-linking, in that changes in distances between two residues can be monitored in real-time, as shown recently (Iino et al., 2005). That study showed that the ATP-induced conformational change takes more than 10 s, from the compact form to the extended form.

Other studies have used antibodies (Johnson and McCarty, 2002) and proteases (Mendel-Hartvig and Capaldi, 1991a,b; Wilkens and Capaldi, 1998) to probe the C-terminal domain of ε. Johnson and McCarty showed that the C-terminus of the chloroplast ε is accessible to antibodies only during ATP synthesis, not ATP hydrolysis. Similarly, the C-terminus of the *E. coli* ε is more sensitive to trypsin digestion in the presence of ADP than with ATP ($+Mg^{2+}$). These studies may have similar limitations in that they require that an enzyme or antibody interact with the coiled-coil domain of ε. Small conformational fluctuations in ε are not likely to be sufficient to be detected by such probes, since for detection they probably require local unfolding of the target protein. Therefore, the chemical labeling approach appears to be more sensitive for the detection of small conformational changes through out the ε subunit.

Based on the results of this study we propose that neither nucleotide binding at catalytic or noncatalytic sites, nor the proton motive force, directly compel the C-terminus of subunit ε to extend. Rather, it is both the availability of a docking site, and the intrinsic instability of the α-helical coiled-coil at the C-terminus of ε that allows the extended conformation to form. The precise conditions under which the extended conformation of ε forms in the *E. coli* ATP synthase remain to be determined. It likely occurs during ATP synthesis, or during inhibition of ATP hydrolysis by ε.

What makes the coiled-coil of the ε subunit inherently unstable? Typical coiled-coils have leucines or other hydrophobic residues at the interface. For example, in the coiled-coil of seryl-tRNA synthetase every eighth residue is a leucine (Belrhali et al., 1994). In comparison, the ε subunit of *E. coli* has mostly alanines at the helical interface. This interaction has been termed an "alanine zipper" (Uhlin et al., 1997). Because of its size, alanine provides a smaller surface area of contact when compared to leucine, and therefore provides a weaker hydrophobic interaction. In addition, the α-helices in ε are somewhat shorter than typical coiled-coils. Helix 1 is about 16 residues long and helix 2 is about 23. The N-terminal coiled-coil of the seryl tRNA synthetase contains helices of more than 30 residues each. These two features result in a weaker helix-helix interface in the ε subunit, and contribute to its propensity for conformational change.

Acknowledgements This work was supported by NIH grant GM-40508 to SBV.

Bibliography

Ackerman SH, Tzagoloff A (2005) Prog Nucleic Acid Res Mol Biol 80:95–133

Aggeler R, Capaldi RA (1996) J Biol Chem 271:13888–13891

Aggeler R, Chicas-Cruz K, Cai SX, Keana JF, Capaldi RA (1992) Biochemistry 31:2956–2961

Aggeler R, Weinreich F, Capaldi RA (1995) Biochim Biophys Acta 1230:62–68

Belrhali H, Yaremchuk A, Tukalo M, Larsen K, Berthet-Colominas C, Leberman R, Beijer B, Sproat B, Als-Nielsen J, Grubel G, et al (1994) Science 263:1432–1436

Boyer PD (1993) Biochim Biophys Acta 1140:215–250

Braig K, Menz RI, Montgomery MG, Leslie AG, Walker JE (2000) Struct Fold Des 8:567–573

Bulygin VV, Duncan TM, Cross RL (1998) J Biol Chem 273:31765–31769

Capaldi RA, Aggeler R (2002) Trends Biochem Sci 27:154–160

Chothia C (1976) J Mol Biol 105:1–12

Dallmann HG, Flynn TG, Dunn SD (1992) J Biol Chem 267:18953–18960

Dimroth P, von Ballmoos C, Meier T (2006) EMBO Rep 7:276–282

Eisenhaber F, Argos P (1993) J Comp Chem 14:1271–1280

Feniouk BA, Suzuki T, Yoshida M (2006) Biochim Biophys Acta 1757:326–338

Gibbons C, Montgomery MG, Leslie AG, Walker JE (2000) Nat Struct Biol 7:1055–1061

Hausrath AC, Capaldi RA, Matthews BW (2001) J Biol Chem 276:47227–47232

Iino R, Murakami T, Iizuka S, Kato-Yamada Y, Suzuki T, Yoshida M (2005) J Biol Chem 280:40130–40134

Iizuka S, Kato S, Yoshida M, Kato-Yamada Y (2006) Biochem Biophys Res Commun 349:1368–1371

Johnson EA, McCarty RE (2002) Biochemistry 41:2446–2451

Kato-Yamada Y, Bald D, Koike M, Motohashi K, Hisabori T, Yoshida M (1999) J Biol Chem 274:33991–33994

Kato-Yamada Y, Noji H, Yasuda R, Kinosita K Jr, Yoshida M (1998) J Biol Chem 273:19375–19377

Kato-Yamada Y, Yoshida M (2003) J Biol Chem 278:36013–36016

Kato-Yamada Y, Yoshida M, Hisabori T (2000) J Biol Chem 275:35746–35750

Long JC, DeLeon-Rangel J, Vik SB (2002) J Biol Chem 277:27288–27293

Mendel-Hartvig J, Capaldi RA (1991a) Biochemistry 30:1278–1284

Mendel-Hartvig J, Capaldi RA (1991b) Biochemistry 30:10987–10991

Pan W, Ko YH, Pedersen PL (1998) Biochemistry 37:6911–6923

Peskova YB, Nakamoto RK (2000) Biochemistry 39:11830–11836

Rodgers AJ, Wilce MC (2000) Nat Struct Biol 7:1051–1054

Schulenberg B, Aggeler R, Murray J, Capaldi RA (1999) J Biol Chem 274:34233–34237

Smith JB, Sternweiss PC (1977) Biochemistry 16:306–311

Suzuki T, Murakami T, Iino R, Suzuki J, Ono S, Shirakihara Y, Yoshida M (2003) J Biol Chem 278:46840–46846

Tang CL, Capaldi RA (1996) J Biol Chem 271:3018–3024

Uhlin U, Cox GB, Guss JM (1997) Structure 5:1219–1230

Vik SB, Cain BD, Chun KT, Simoni RD (1988) J Biol Chem 263:6599–6605

Wilkens S, Capaldi RA (1998) J Biol Chem 273:26645–26651

Wilkens S, Dahlquist FW, McIntosh LP, Donaldson LW, Capaldi RA (1995) Nat Struct Biol 2:961–967

Xiong H, Vik SB (1995a) J Biol Chem 270:23300–23304

Xiong H, Vik SB (1995b) J Bacteriol 177:851–853

Xiong H, Zhang D, Vik SB (1998) Biochemistry 37:16423–16429

Zhang D, Vik SB (2003) J Biol Chem 278:12319–12324

Zhang Y, Fillingame RH (1995) J Biol Chem 270:24609–24614